Werk

Jahr: 1984
Kollektion: fid.geo
Signatur: 8 Z NAT 2148:55
Digitalisiert: Niedersächsische Staats- und Universitätsbibliothek Göttingen
Werk Id: PPN1015067948_0055
PURL: http://resolver.sub.uni-goettingen.de/purl?PPN1015067948_0055

LOG Id: LOG_0027
LOG Titel: Ground-satellite coordinated study of the April 5, 1979 events: flux variations of energetic particles and associated magnetic pulsations
LOG Typ: article

Übergeordnetes Werk

Werk Id: PPN1015067948
PURL: http://resolver.sub.uni-goettingen.de/purl?PPN1015067948
OPAC: http://opac.sub.uni-goettingen.de/DB=1/PPN?PPN=1015067948

Contact

Niedersächsische Staats- und Universitätsbibliothek Göttingen
Georg-August-Universität Göttingen
Platz der Göttinger Sieben 1
37073 Göttingen
Germany
Email: gdz@sub.uni-goettingen.de

J Geophys (1984) 55:120–133

Journal of Geophysics

Ground-satellite coordinated study of the April 5, 1979 events: flux variations of energetic particles and associated magnetic pulsations

U. Wedeken[1], B. Inhester[1], A. Korth[2], K.-H. Glaßmeier[3], R. Gendrin[4], L.J. Lanzerotti[5], H. Gough[6]★, C.A. Green[7], E. Amata[8], A. Pedersen[9], G. Rostoker[10]

[1] Institut für Geophysik, Universität Göttingen, D-3400 Göttingen, Federal Republic of Germany
[2] Max-Planck-Institut für Aeronomie, D-3411 Katlenburg-Lindau, Federal Republic of Germany
[3] Institut für Geophysik, Universität Münster, D-4400 Münster, Federal Republic of Germany
[4] Centre de Recherches en Physique de l'Environnement, CNET, F-92131 Issy-les-Moulineaux, France
[5] AT & T Bell Laboratories, Murray Hill NJ 07974, U.S.A.
[6] Department of Physics, University of York, York Y01 5DD, Great Britain
[7] Institute of Geological Sciences, Geomagnetism Unit, Edinburgh EH9 3LA, Great Britain
[8] Istituto di Fisica dello Spazio Interplanetario, CNR, I-00044 Frascati, Italy
[9] Space Science Department of ESA, ESTEC, NL-2200 AG Noordwijk, The Netherlands
[10] Department of Physics, University of Alberta, Edmonton, Canada T6G 2J1

Abstract. About half an hour after the onset of a substorm expansion phase, the geostationary satellite GEOS-2 in the afternoon sector observed energetic ions that were injected on the nightside of the magnetosphere. With the arrival of these ions, wave activity started and the flux of energetic particles varied in the pc5 period range. Largest modulations occurred at pitch angles around 90°. The total magnetic induction and the electron flux had minima at the times of ion flux maxima and vice versa. The GEOS-2 data allowed the estimation of the $\beta_\perp$-value, the ion temperature anisotropy and the perpendicular wave number. The wavelength is of the order of 1,500 km and, together with the observed frequency, the dispersion relation of a drift mirror mode is roughly satisfied if the drift is essentially given by the magnetic field gradient.

We found no strong correlation between the drift mirror wave and shear Alfvén waves, although GEOS-2 also observed large transverse magnetic and electric field oscillations. These transverse magnetic field disturbances may partly be associated with the drift mirror wave and partly be due to a surface wave generated at the outer boundaries of the magnetosphere. On the other hand, the electric field oscillations only correlate with the pc5 pulsations observed at the ground, and this coherency is very high. We assume that the pc4–5 pulsations detected on the ground between $L \simeq 2.3$ and $L \simeq 6.3$ are due to field line resonances driven by surface waves in the magnetopause region. It is likely that GEOS-2 was on L-shells outside the dominant pc5 resonance region and that these pc5 pulsations were not coupled to the drift mirror wave.

Key words: Drift mirror instability – Pc4–5 pulsations – Mode coupling – Field line resonance

★ *Now at:* British Antarctic Survey, NERC, Cambridge CB3 0ET, Great Britain

Offprint requests to: U. Wedeken

Introduction

Modulations of the magnetic field in the hydromagnetic regime are fairly well understood in many cases (e.g. Lanzerotti and Southwood, 1979). Theoretical concepts regarding hydromagnetic waves in the magnetosphere have been reviewed recently by Southwood and Hughes (1983). The transverse (or shear Alfvén) mode and the fast (or compressional) mode are generally discussed in terms of field line resonances in a cold plasma in the dipole field of the earth (e.g. Walker, 1980).

The characteristics of these low frequency waves ($f \lesssim 0.5$ Hz) change drastically in the presence of a hot component of the magnetospheric plasma. When the plasma β (ratio of gas to magnetic pressure) is high ($0.1 \lesssim \beta \lesssim 1$, e.g. in the storm-time ring current region), large compressional hydromagnetic waves in the pc5 range (periods $\sim$150–600 s) are often observed with simultaneous variations of particle fluxes (see the early observations by Brown et al., 1968; Sonnerup et al., 1969). One of the high-β plasma instabilities invoked to explain some of the observations is the drift mirror instability, in which the classical mirror instability is modified by gradients in the magnetic field and the hot plasma density (Hasegawa, 1969; Lanzerotti et al., 1969). The drift mirror waves show large compressional and smaller transverse magnetic oscillations (e.g. Walker et al., 1982). Lin and Parks (1978) proposed that the storm time pc5 pulsations might be caused by the coupling of Alfvén and unstable drift mirror waves. Walker et al. (1982) showed how the drift mirror mode is coupled to a guided poloidal mode in a dipole field geometry. Patel et al. (1983) presented a drift wave model containing coupled drift compressional, drift mirror, and shear Alfvén waves in a high-β plasma. They calculated relative wave amplitudes from the model and found high growth rates for the drift mirror instability. However, the model developed by Patel et al. (1983) provided no correlations between theory and obser-

vations regarding relative wave amplitudes of a drift mirror instability.

A drift wave instability of a compressional hydromagnetic wave (also called drift compressional instability) occurs when the Alfvén velocity is smaller than the hot proton drift speed associated with diamagnetic or gradient-curvature-B drift (Lanzerotti and Hasegawa, 1975). A theory of localized compressional hydromagnetic waves resulting from a field line resonance in a hot inhomogenous plasma was given by Southwood (1977). In this theory, the compressional component ($b_{||}$) just adds to the transverse signal and the magnitude of $b_{||}$ depends on the β-value.

A typical problem of interpreting observations of simultaneous particle and field fluctuations is the lack of sufficiently detailed information to prove conclusively the criteria for a special instability. Kremser et al. (1981) studied simultaneous quasi-periodic variations of energetic particle fluxes and the geomagnetic field in the pc5 period range. The events were observed on board the geostationary satellite GEOS-2, and a reasonable agreement with the predictions of the drift mirror instability was found. Studies of a special event were extended by Walker et al. (1982), who used data from GEOS-2 and the Scandinavian Twin Auroral Radar Experiment (STARE). This investigation suggested that a guided poloidal Alfvén wave coupled to a particle-driven drift mirror wave. In a recent report by Walker et al. (1983), electric field data from GEOS-2 were added in order to model the fields of these waves.

In this paper we study a pc5 event similar to the 'out-of-phase' events (i.e. electron flux in phase with magnetic field intensity and in anti-phase with ion flux) analysed by Kremser et al. (1981) and Walker et al. (1982, 1983). We also use GEOS-2 measurements of energetic particles and the magnetic and electric fields, including ULF waves and various plasma parameters. Ground-based magnetometer data complete the observation data base. Riometer and STARE data were also inspected. The selected event occurred during an extensively studied time interval which was a topic of the 'Sixth Workshop on IMS Observations in Northern Europe' held at Windsor, England, in May 1983.

Instrumentation and recording sites

The day studied (April 5, 1979) belongs to a geomagnetically very active interval which occurred during the IMS (International Magnetospheric Study) and data from a large number of ground magnetometers were available. Table 1 lists the positional parameters of the European stations used in this study.

On the day of interest, the geostationary satellite GEOS-2 was located at a geographic longitude of 37.5 °E, a geomagnetic latitude of about 3 °S and a distance of $6.62R_E$ from the centre of the earth (R_E = earth radius). At 1200 UT the approximate ionospheric footprint of the GEOS-2 magnetic field line was located about 200 km west of KUN (J.I. Vette, personal communication). However, the uncertainty in this determination is large because of the distortion of the magnetosphere which could not fully be taken into account for this active day.

Magnetic field data from GEOS-2 (experiment S-331) are available in the VDH coordinate system (e.g. Greenwald et al., 1981), while the measured quasi-static electric fields (experiment S-300) are given in the SDB coordinate system (Pedersen and Grard, 1979). These field data from GEOS-2 were transformed into a mean-field-aligned coordinate system: v points outwards, away from the rotation axis of the earth and v is perpendicular to the mean direction of the magnetic field **B**, φ is the azimuthal component, positive eastwards, and μ is the field-aligned component. Note that the direction of the electric field component $E_\varphi(E_v)$ does not exactly coincide with the direction of $B_\varphi(B_v)$ because the electric field components are nearly perpendicular to the actual direction of **B**, while B_φ and B_v are perpendicular to the mean direction of **B** (averaged over the largest pulsation period). However, this difference in the directions is $\lesssim 5°$ for this case study (i.e. it can be neglected) and we use the $v\varphi\mu$ coordinate system for both the electric and magnetic field components.

Energetic electrons and ions are measured with the GEOS-2 magnetic spectrometer (experiment S-321; Korth et al., 1978), and integral and differential particle

Table 1. List of European ground stations

Station	Code	Geographic coordinates		Geomagnetic coordinates		CGM[a] (UT)	L-value
		Latitude	Longitude	Latitude	Longitude		
Kunes	KUN	70.4	26.5	66.6	123.3	2115	6.3
Kevo	KEV	69.8	27.0	66.0	122.9	2116	6.0
Ivalo	IVA	68.6	27.5	64.8	121.9	2119	5.5
Esrange	ESR	67.9	21.1	64.5	116.2	2139	5.4
Martti	MAR	67.5	28.3	63.7	121.4	2120	5.1
Kuusamo	KUU	65.9	29.1	62.1	120.5	2122	4.6
Faroes	FA	62.0	−6.8	61.6	84.8	2316	4.4
Lerwick	LE	60.1	−1.2	58.9	88.6	2304	3.8
Durness	DU	58.6	−4.8	57.7	83.7	2318	3.5
Eskdalemuir	ES	55.3	−3.2	54.1	82.9	2318	2.9
York	YO	54.0	−1.1	52.6	84.2	2314	2.7
Hartland	HA	51.0	−4.5	49.9	79.0	2330	2.4
Kartoffelstein	KST	51.6	10.0	48.9	93.7	2246	2.3

[a] Estimated corrected geomagnetic midnight (CGM) for day 95 (Montbriand, 1970)

data are used. Electron and ion fluxes with energies 16–300 keV and 27 keV–3.3 MeV, respectively, are measured. Unfortunately, the ion detector P2, covering a large part of the pitch angle range perpendicular to **B**, suffered interference from sunlight during parts of each satellite rotation.

ULF/ELF magnetic fields at GEOS-2 are recorded with search coil magnetometers (experiment S-300; Perraut et al., 1978). The three orthogonal sensors are oriented parallel to the spin axis (*BZ*), which roughly corresponds to the direction of **B**, and in the plane perpendicular to it. The measurements of the perpendicular field components are transformed into the right-handed (*BR*) and left-handed (*BL*) circularly polarized components.

Thermal and suprathermal ion fluxes in the direction nearly perpendicular to **B** are recorded on board GEOS-2 by the Ion Composition Experiment (ICE, S-303; Geiss et al., 1978).

Data from two satellites outside the magnetosphere were available: ISEE-3 was positioned at the sub-solar libration point ($X=221\,R_E$, $Y=-101\,R_E$, $Z=3\,R_E$, geocentric solar ecliptic coordinate system), and IMP-8 at 1000 UT was situated at a distance of $36.5\,R_E$ on the evening side ($X=-5.7R_E$, $Y=32.5R_E$, $Z=15.5R_E$).

For more details about the satellites, the different magnetometer networks, STARE and the Finnish riometer chain from which data are used in this study, see 'The IMS Source Book' (Russell and Southwood, 1982).

General geomagnetic disturbance situation

A storm sudden commencement (ssc) on April 1, 1979, initiated a sequence of magnetically disturbed days, with the daily ΣKp always greater than 32+. Figure 1 displays, in the lower two panels, the geomagnetic disturbance situation for the interval April 3, 1979, 2100 UT until April 5, 1979, 2100 UT. The equatorial ring current intensity, as measured by the *Dst* index, increased significantly, and on April 4, around 0400 UT, the hourly *Dst* values decreased to −200 nT. In conjunction with this, the auroral electrojets (as indicated by the auroral magnetic indices *AU* and *AL*) were significantly intensified. The recovery phase began at this time, and by the time the ring current had decayed to a *Dst* value of −62 nT, another interplanetary shock arrived on April 5 at 0156 UT.

Magnetograms of the satellite ISEE-3 (from the data pool tape) and the Scandinavian station Kevo (KEV) for the time interval 0100 to 2100 UT are shown in the two upper panels of Fig. 1. ISEE-3 recorded a large magnitude of the interplanetary magnetic field (IMF) for most of the time interval of interest. Magnitudes of up to 40 nT and sustained intervals of strong northward IMF ($B_Z>0$) can be observed. They should be accompanied by a strong solar wind flow. With a delay of approximately 1 h, IMP-8 recorded a similar shape of the IMF (not shown). Assuming a propagation of the solar wind along the sun-earth line, this delay would imply a solar wind velocity of nearly 400 km/s.

In the vicinity of the earth's magnetosphere the time interval 0700–1030 UT appears to be the only interval in which the IMF had some periods with a southward

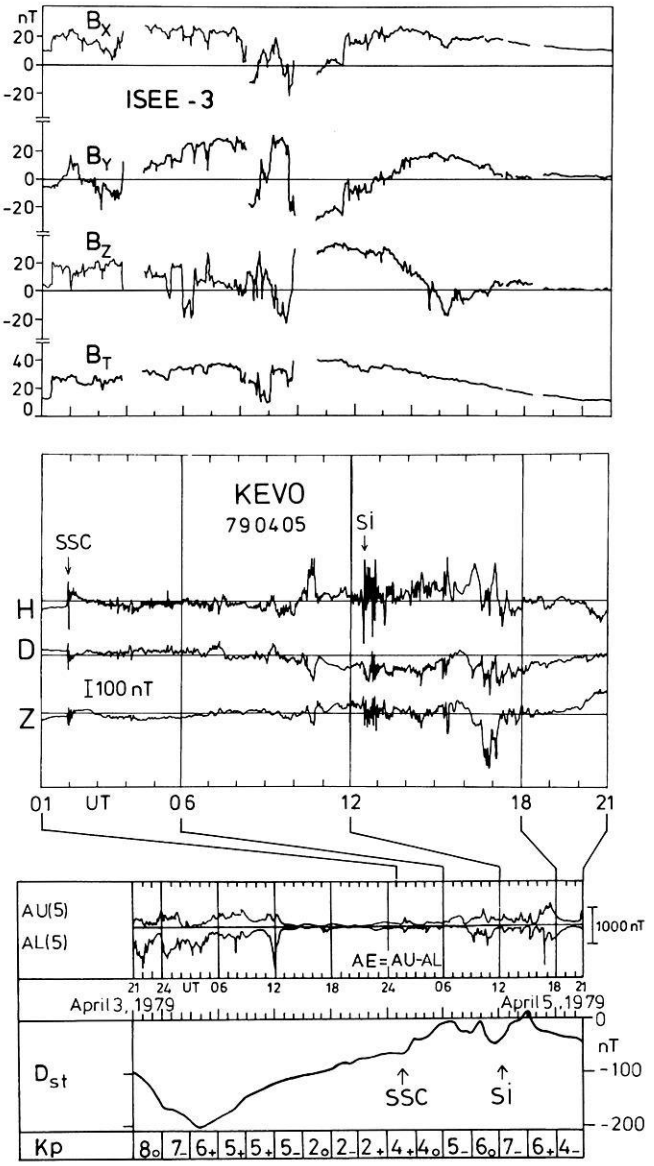

Fig. 1. The *top traces* show the interplanetary magnetic field recorded by ISEE-3 (components B_X, B_Y, B_Z, GSM-system, and the total field strength B_T) on April 5, 1979, 0100–2100 UT. The *middle* and *lower traces* present the level of geomagnetic activity by a magnetogram of the station Kevo in northern Finland, the *AU* and *AL* indices, the hourly *Dst* values, and the *Kp* indices. *AU* and *AL* are taken from the IAGA Bulletin No. 32j, 1980 (common-scale magnetograms April 3–5, 1979, page 77)

component ($B_Z<0$). On the nightside the Alberta array observed significant substorm activity at this time. This is shown in Fig. 2, where the records from the Alberta array are displayed for an interval corresponding to about 1530–0530 MLT.

Until about 1000 UT no strong electrojet occurred in northern Scandinavia (Fig. 1). Between 0925 and 0950 UT, i.e. around local noon, GEOS-2 was in the magnetosheath. At this time the sonograms of the ULF waves (not shown) indicate very intense broadband electromagnetic noise which is usually observed when GEOS crosses the magnetopause (Gendrin, 1983). In our case the short entrance into the magnetosheath is

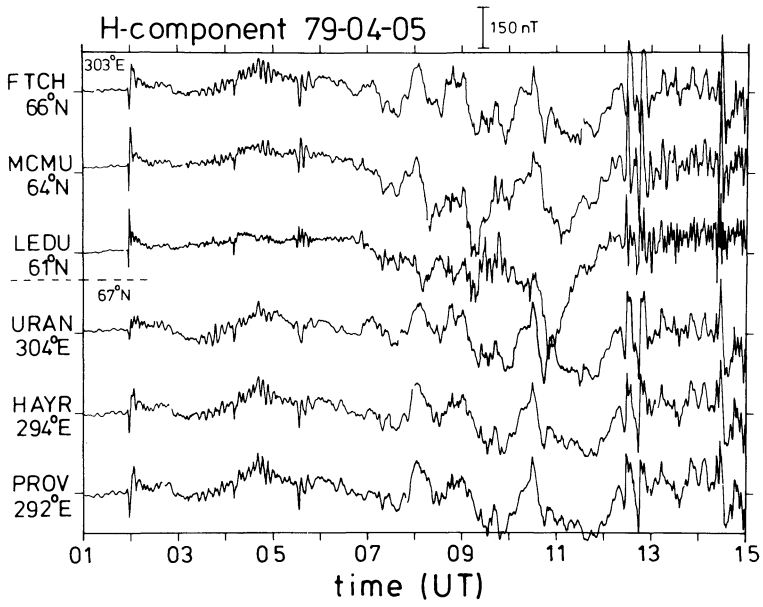

Fig. 2. Magnetometer records of the H component from the Alberta array. The *upper three records* represent a north-south chain near 303° E geomagnetic longitude, while the *lower three records* display an east-west chain around 67° N geomagnetic latitude

verified by simultaneous large decreases of the ion intensities and the energetic electron fluxes observed by GEOS-2.

A northward turning of the IMF at 1030 UT (at ISEE-3 nearly 1 h earlier) probably triggered the last substorm expansion phase. At that time the stations of the Alberta array, which were then near 0130 MLT, observed a sharp decrease of the H component (Fig. 2). Rostoker (1983) has shown that after an interval of sustained southward IMF, a northward turning of the IMF can trigger the expansive phase of a large substorm.

Starting at 1015 UT and lasting until about 1100 UT, strong geomagnetic variations and pc2-5 pulsations were also recorded in Europe (partly visible in Fig. 1). Between 1110 and 1115 UT a small isolated pc2 wave packet occurred in Scandinavia north of $L=5$. Of special interest is the time interval 1121-1225 UT, with large compressional pc5 waves at GEOS-2 (see next section).

At 1225 UT a sudden impulse (si) triggered new pulsation activity and the Kp index increased to 7. After the si the IMF was clearly steady, with a northward component and a total magnitude of about 30 nT (IMP-8 data). The prominent pulsation activity (Figs. 1 and 2) seems to be a signature of this large IMF and the accompanying solar wind flow. The auroral oval must have been pushed far equatorward of its normal position. The most intense pulsation activity is found between about $L=4.5$ and $L=5.5$. GEOS-2 again, for a time, probably entered the magnetopause boundary layer.

In summary, we note that a large IMF was probably associated with a strengthened solar wind flow which forced the auroral oval to lower latitudes. Both the IMF and the solar wind flow strongly influenced the magnetopause region, while the inner magnetosphere had stored a large amount of free energy.

The ssc observed at 0156 UT with associated events and the very interesting pc5 events occurring after 1225 UT will be studied in two future papers.

Observations between 1030 and 1225 UT

Particle data

Drifting high energy ions, probably injected near 1030 UT in the midnight region in connection with the onset of the substorm expansion phase mentioned above, arrived at GEOS-2 between about 1045 and 1115 UT on April 5, 1979. Figure 3 shows the differential ion intensities in the energy range 36-403 keV for the pitch angle range $80°\pm5°$. The energy dispersion related to the drift of the ions is clearly visible, and the enhancement of the flux in the different energy channels is marked by a dotted line. The counting rate of channel 9 (ions with energy ~200 keV) increases at 1047 UT (around 1317 MLT), for example. Ions of such energy have a drift period of 34 min in the dipole field. Assuming an injection at local midnight (cf. McPherron, 1979), it should have occurred around 1030 UT.

Figure 3 also shows that strong intensity variations of the ion fluxes start around 1120 UT and they occur simultaneously over the energy range from 36 to about 150 keV.

The energetic electrons showed no energy dispersion. The probable cause is the loss of the electrons in the noon region at the magnetopause. Note that GEOS-2 entered the magnetosheath when it was located near local noon.

Between 1115 and 1215 UT the electron plasma density at GEOS-2 varied little around 15 cm^{-3} (B. Higel, personal communication). In the energy range $E=0.1$-15 keV, the O^+ ion density increased from ~0.7 cm^{-3} (1115 UT) to ~1.2 cm^{-3} (1150 UT) and ~2.1 cm^{-3} (1200 UT; M. Stokholm, personal communication). The total number density of the electrons in the energy range 50-500 eV detected by GEOS-2 reached a minimum of ~0.06 cm^{-3} between 1100 and 1225 UT, while the cold proton density (energies <5 eV) maximized with ~5 cm^{-3} (G. Wrenn, personal communication).

The ion $\beta_\perp$-value, $\beta_\perp=2\mu_0 P_\perp/B^2$ (ratio of perpendicular plasma pressure to magnetic pressure), at the po-

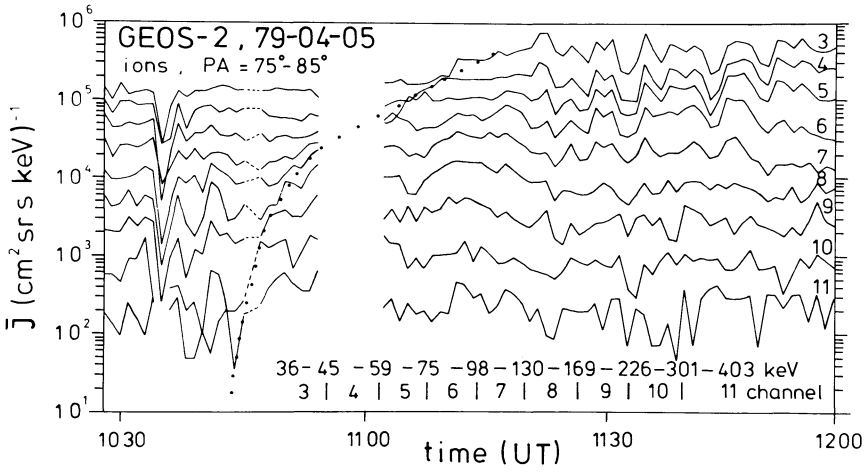

Fig. 3. Intensity of ions with pitch angles (PA) 75°–85° measured in nine energy channels on GEOS-2 between 1030 and 1200 UT. The arrival times for different energies of ions are marked by a *dotted line*

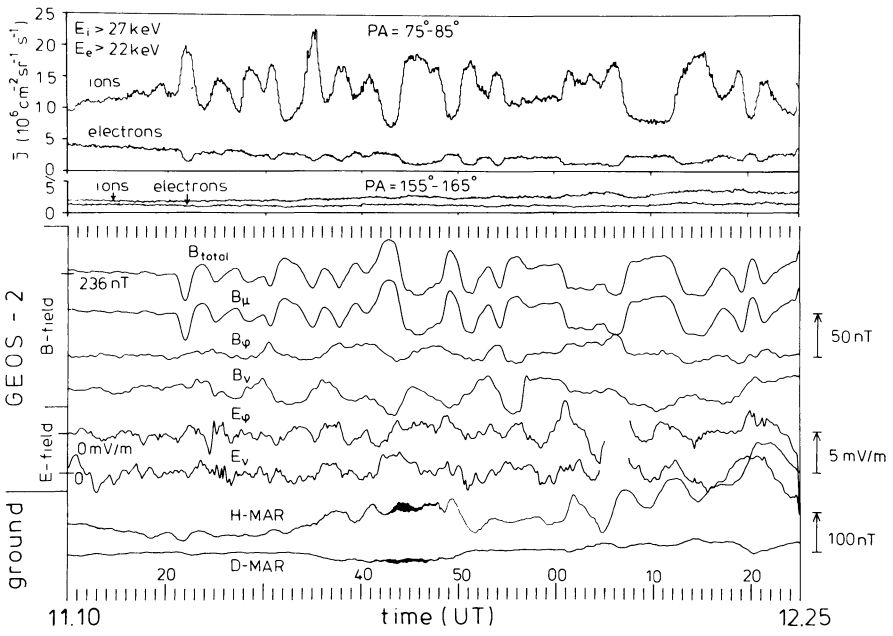

Fig. 4. Satellite-ground comparison *At the top* the integral fluxes of ions and electrons with pitch angles 75°–85° and 155°–165° are shown on a linear scale. *In the middle* the total magnetic field, three components of the magnetic field, and two components of the electric field recorded at GEOS-2 are presented. *At the bottom* the pulsation records of the ground station Martti (MAR) near Sodankylä are displayed. Note the pc2 wave packet at MAR around 1145 UT

sition of GEOS-2 has been estimated from the ion flux measurements of the S-303 experiment ($E = 0.1$–15 keV, pitch angle $\sim 90°$) and the S-321 experiment ($E = 28$–169 keV, nearly all pitch angles). This was done in the way described by Roux et al. (1982), following on the work of Gurgiolo et al. (1979) for the interval 1133:37–1134:37 UT, at which time the flux of energetic ions with pitch angles near 90° was close to the mean value (= average over approximately 0.5 h) in the course of a strong increase (see Fig. 3). With the measured magnetic field strength $B = 238$ nT we calculated

$$\beta_\perp = 0.22.$$

The contribution to $\beta_\perp$ from the energy gap 16–27 keV had to be interpolated and amounted to 25% of the total perpendicular plasma pressure. The $\beta_\perp$-value increases to $\beta_\perp \simeq 0.5$ at times of largest ion intensity maxima and decreases to $\beta_\perp \simeq 0.1$ at the times of lowest ion pressure.

From the pitch angle distributions we could estimate the temperature anisotropy of the ions $A = (T_\perp/T_\parallel) - 1$, which varied in the range 0.3–1.

Indications of a drift mirror instability

The time interval 1121–1225 UT is of special interest as very pronounced pc5 activity is seen in both the particle data and the magnetic field measured by GEOS-2 (Fig. 4). At the ground, a pronounced pc5 event with considerable amplitudes in the H component is observed only between 1201 and 1215 UT (Fig. 4). This event consists of about three oscillations with a period near 300 s. The electric field at GEOS-2 clearly shows this pc5 event, although a data gap covers the main part of the second oscillation.

The magnetic field intensity measured by GEOS-2 shows similar fluctuations in the pc5 period range as the energetic particles with pitch angles near 90°, and the ion flux oscillates exactly in opposite phase to the total magnetic field while the electron flux is just in phase with these field fluctuations. Also, the ion intensity at pitch angles near 90° is strongly increased as a result of the injection near 1030 UT mentioned earlier, followed by the azimuthal drift (Fig. 3). The peak-to-peak amplitudes of the intensity variations of the ions with pitch angles near 90° can reach the mean

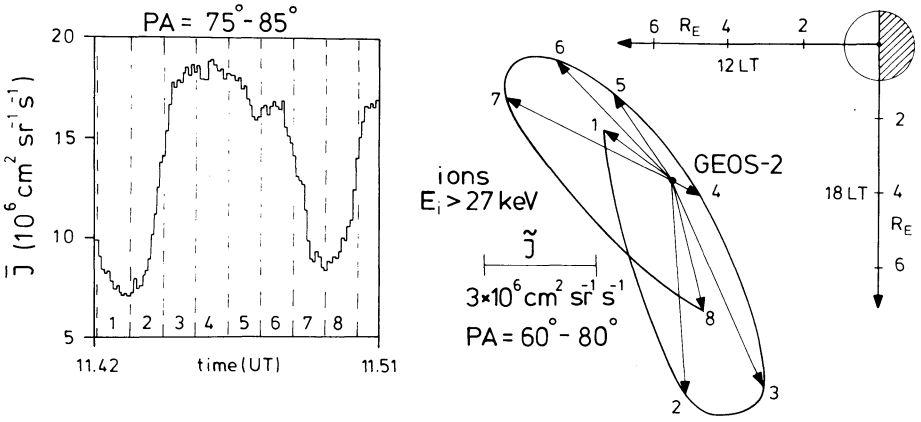

Fig. 5. Integral ion flux $\bar{J}$ averaged over one spin period (*left panel*) and azimuthal directions of the ion density gradients in the approximately equatorial plane (*right panel*). The eight gradients correspond to eight subsequent time intervals between 1142 and 1151 UT which are denoted by numbers and shown in the *left panel*. The direction of the highest azimuthal ion flux is rotated clockwise by 90° in order to give an equivalent density gradient vector. The length is given by the difference of the highest azimuthal flux and the flux in the opposite direction which mostly agrees with the lowest azimuthal flux. The final points of the vectors are connected by a curve in order of the interval number

value of the total intensity (Fig. 4). Note that the fluxes of energetic particles with pitch angles $160° \pm 5°$ show only small variations.

The large mean value (~ 240 nT) of the total magnetic field indicates a rather compressed magnetosphere. The periods of the pc5 fluctuations observed on GEOS-2 were examined by dynamic spectra and they vary between 200 and 400 s with peak-to-peak amplitudes up to 70 nT. The largest change of the magnetic field (between 1143 and 1145 UT) is accompanied by extremely large pc2 waves (periods ~ 10 s), reaching amplitudes of 24 nT peak-to-peak in H at the ground station MAR (see Fig. 4).

The observed long-period event is similar to the "out-of-phase events" discussed by Kremser et al. (1981), and the interpretation for their event - a possible drift mirror instability which is associated with drifting energetic ion bunches - may also apply here. However, the observed values for $\beta_\perp$ and the anisotropy, A, do not quite reach the linear instability condition given by Hasegawa (1969).

Kremser et al. (1981) reported that for pitch angles $\alpha < 90°$ ($\alpha > 90°$) the variations of the electron intensity J_e were out of phase with the ion intensity variations for $dJ_e/d\alpha < 0$ ($dJ_e/d\alpha > 0$) in the range $50° \lesssim \alpha \lesssim 140°$, i.e. J_e showed a minimum at $\alpha \simeq 90°$ (butterfly distribution). Such an electron distribution is interpreted by Lanzerotti et al. (1969) as an influence of the drift mirror instability. Consequently, we examined the pitch angle distributions of our out-of-phase event. A butterfly distribution was found for electrons with energies > 20 keV for all times, except the times of J_e maxima (=times of ion intensity minima). At these times, J_e showed a maximum near $\alpha = 90°$. Therefore, the variations of J_e were most pronounced at pitch angles near 90°. For $\alpha \gtrsim 130°$, J_e showed a small maximum at the times of ion intensity maxima, i.e. for these large pitch angles the electron flux varied in anti-phase to the variations of the magnetic field strength. This was also found by Kremser et al. (1981).

For the time interval between 1142 and 1150 UT, the dependence of the ions with energies > 27 keV and pitch angles near 90° on the azimuth around the magnetic field line has been studied. Figure 5 shows the result, which can roughly be interpreted as a monochromatic and spatially homogeneous density wave travelling past GEOS-2 in an almost azimuthal direction. In this ideal case, the ion flux J seen on board GEOS-2 should vary with time and azimuth as

$$J(\varphi, t) = \bar{J}(t) + \tilde{J}(t) \sin(\varphi - \varphi'), \tag{1}$$

where $\bar{J}(t) = J_0 + J_1 \cos \omega t$ is the azimuthally averaged ion flux given in the left hand side of Fig. 5, and $\tilde{J}(t) = J_2 \sin \omega t$ is the azimuthal variation of the flux relative to the azimuth angle φ' of the wave's **k**-vector. $\tilde{J}$ is proportional to the wave field density gradient $k_\perp \delta N_h$, where $k_\perp$ is the wave number perpendicular to **B** and δN_h is the variation of the hot ion number density which is proportional to J_1.

The right hand side of Fig. 5 is a polar plot of $\tilde{J}(t)$ vs $\varphi'(t)$, the values of which were obtained by fitting the observed azimuth-dependent ion flux for each instance to Eq. (1). An eastward-directed ion density gradient during the flux increase (intervals 2, 3, 8) and a westward-directed gradient during the flux decrease (intervals 5–7) is observed, which indicates a westward-directed phase velocity. The fact that we observe elliptic rather than a linear polarization indicates that the wave does not possess a definite **k**-vector, but rather consists of drifting density bunches.

We can also estimate the magnitude of the dominant perpendicular wave number $k_\perp$ from the observations. With the above idealized description of the wave form, and further assuming a Maxwell distribution for the ions, we derive in the Appendix a relation between the ratio of the flux variation amplitudes J_1 and J_2 to the wave number $k_\perp$, the ion temperatures $T_\parallel$, $T_\perp$, and the energy E above which the ion flux is measured at the pitch angle α:

$$\frac{J_2}{J_1} = \frac{k_\perp}{\Omega} (2T/m_i)^{1/2} \cdot \sin\alpha \, \frac{\pi^{1/2}(1-\Phi) e^{E/T} + (E/T)^{1/2} + \frac{2}{3}(E/T)^{3/2}}{\frac{2}{3}(1+E/T)}. \tag{2}$$

Here, $T = T_\perp/(1 + A\cos^2\alpha)$ is the temperature of ions with pitch angle α, $(T/m_i)^{1/2}$ is their thermal speed, A is their temperature anisotropy, Ω is the proton gyrofrequency and Φ is the error function at the argument of $(2E/T)^{1/2}$. If we substitute the observed values $E = 27$ keV, $\alpha = 70°$, $A = 0.6$, and $T_\perp = 25$ keV, we obtain

$$\frac{J_2}{J_1} \simeq 2.0 \frac{k_\perp}{\Omega}(T_\perp/m_i)^{1/2},$$

whereas the observed amplitudes of the azimuthal and temporal flux variation (see Fig. 5) gives a value of 0.55 ± 0.05 for the left hand side. We therefore obtain a wave number in terms of thermal ion gyroradii ρ_i of

$$k_\perp \rho_i = \frac{k_\perp}{\Omega}(T_\perp/m_i)^{1/2} \simeq 0.28. \tag{3}$$

The measured magnetic field strength, $B = 240$ nT, leads to $\Omega = 23\ s^{-1}$, and therefore we obtain $k_\perp \simeq 4.2 \times 10^{-3}\ km^{-1}$ or a wavelength of $\lambda_\perp \simeq 1{,}500$ km (~ 22 times ρ_i). We argue that this value of $k_\perp$ is representative for the main part of the event since J_2/J_1 does not vary appreciably.

Equation (3) plays a decisive role in Hasegawa's (1969) theory on the drift mirror instability. He has calculated the dispersion of the drift mirror wave to be

$$\omega_D = \frac{T_\parallel}{m_i}\frac{k_\perp}{\Omega}\kappa, \tag{4}$$

where ω_D is the angular drift wave frequency of energetic protons. The parameter κ is either the hot plasma density gradient, $d(\ln N_h)/dr$, or the dipole magnetic field gradient, $d(\ln B)/dr$. If we use Eq. (3) in Eq. (4) and substitute $\kappa = d(\ln B)/dr \simeq 3/(6.6 R_E)$, we obtain an angular frequency $\omega_D \simeq 19 \times 10^{-3}\ s^{-1}$ (period 330 s).

Now we estimate ω_D by using the ambient gradient of the hot ion density which we estimate from the relative displacement of the centre of the polarization ellipse from the origin of the gradients (right panel of Fig. 5)

$$\frac{\nabla N_h}{k_\perp \delta N_h} \simeq 0.2, \tag{5}$$

and from the relative amplitude of the azimuthally averaged ion flux variation (left panel of Fig. 5)

$$\frac{\delta N_h}{N_h} \simeq 0.4. \tag{6}$$

The corresponding angular drift wave frequency, ω_N, then follows from

$$\omega_N = \frac{T_\perp}{m_i}\frac{k_\perp}{\Omega}\frac{\nabla N_h}{N_h} = \frac{k_\perp^2 T_\perp}{\Omega^2 m_i}\frac{\nabla N_h}{k_\perp \delta N_h}\frac{\delta N_h}{N_h}\Omega \tag{7}$$

(cf. Lin and Parks, 1978). If we use Eqs. (3), (5) and (6) and substitute $\Omega = 23\ s^{-1}$, we obtain $\omega_N \simeq 144 \times 10^{-3}\ s^{-1}$ (period 44 s).

In the geocentric solar ecliptic (GSE) coordinate system GEOS-2 moves eastward with $v_{GEOS} = 3$ km/s. Therefore, the angular frequencies observed by GEOS-2 (ω_{obs}) have to be changed by the GEOS-2 Doppler shift before we can compare them with the estimated drift frequencies. In the stationary GSE-system we obtain

$$\omega_{obs}^{GSE} = \omega_{obs} - k_\perp v_{GEOS}. \tag{8}$$

A positive value of ω_{obs}^{GSE} indicates a westward propagation of the wave. ω_{obs} is in the range of 16×10^{-3}–$31 \times 10^{-3}\ s^{-1}$. Therefore, we obtain $3 \times 10^{-3}\ s^{-1} \lesssim \omega_{obs}^{GSE} \lesssim 19 \times 10^{-3}\ s^{-1}$ (period range ~ 330–2,100 s), and ω_D agrees with the upper limit of this observed frequency range. According to Patel and Migliuolo (1980) the presence of hot heavy ions reduces ω_D. The effect of the observed abundance of O^+ ions was only considered in the calculation of $\beta_\perp$.

The diamagnetic drift frequency, ω_N, is much larger than ω_{obs}^{GSE}. We therefore assume that the westward-directed guiding centre drift in our case is the important parameter to describe the drift mirror instability (cf. Walker et al., 1982; Ng and Patel, 1983). This guiding centre drift principally agrees with the gradient-B drift because the resonant ions with pitch angles near 90° show no significant curvature-B drift ($v_\parallel \simeq 0$). Note that the diamagnetic drift is eastward since ∇N_h is directed outwards, but a westward-propagating wave is observed.

According to Hasegawa (1969) the expected ratio $\delta P_\perp/\delta P_\parallel$ of the variations of perpendicular and parallel pressures can be estimated by

$$\frac{\delta P_\perp}{\delta P_\parallel} \simeq 2\frac{v_\perp^2}{v_\parallel^2} = 2\frac{T_\perp}{T_\parallel}, \tag{9}$$

leading to $\delta P_\perp/\delta P_\parallel \simeq 3$ in our case, where $T_\perp/T_\parallel \simeq 1.6$. But we observed a ratio $\gtrsim 10$ between the flux modulations with pitch angles near 90° and above 150°.

Hasegawa (1969) has shown that the perturbations in the pressure and the magnetic field strength are related by

$$\frac{\delta P_\perp}{2P_\perp} \simeq \frac{\delta N_h}{2N_h} \simeq \left(1 - \frac{T_\perp}{T_\parallel}\right)\frac{b_\parallel}{B}, \tag{10}$$

where $P_\perp$ is the perpendicular pressure in the unperturbed state. Therefore, if $T_\perp > T_\parallel$, δN_h and $b_\parallel$ in fact are in anti-phase. If $T_\perp/T_\parallel = 1.6$, $\delta N_h/N_h = 0.4$, and $B = 240$ nT is substituted, then $b_\parallel \simeq 80$ nT is obtained, about 3 times larger than observed.

Long-period Alfvén waves

GEOS-2 observations. If we assume a drift mirror instability, a guided poloidal wave should be coupled to the drift mirror wave (cf. Walker et al., 1982).

The lower seven traces displayed in Fig. 4 have been bandpass filtered (period range 200–600 s) to allow a better comparison of the waves in the pc5 period range. Figure 6 shows the filtered data. Now the large oscillations of the radial magnetic field component B_v (up to 50 nT peak-to-peak) are more visible, with periods increasing from 350 s around 1130 UT to ~ 470 s near 1220 UT. The peak-to-peak correlation between B_v and the field-aligned component, B_μ, or the azimuthal electric field component, E_φ, is very poor. The complex shape of B_v does not allow a clear phase comparison with other traces. Nevertheless, power spectra calculated

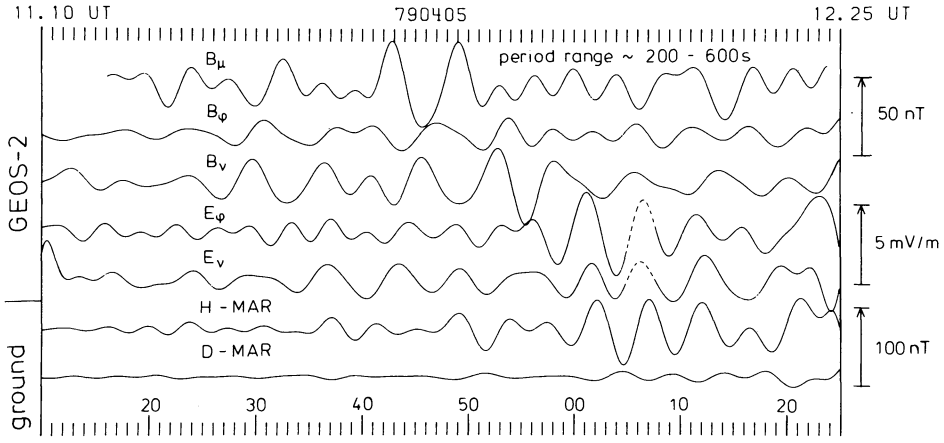

Fig. 6. Bandpass-filtered data of the seven lower time series from Fig. 4 (cut-off periods 200 and 600 s). The data gap in the electric field is filled by interpolated values (*dashed lines*)

for the time interval 1120–1220 UT indicate a phase difference of $180° \pm 40°$ between B_μ and B_v (period ~ 400 s). Furthermore, B_φ leads B_μ by $95° \pm 50°$ for periods near 400 s. In the plane perpendicular to **B** the relatively small polarized part of the signals indicates a right-handed sense of polarization.

The cross-correlation studies of electric and magnetic field components measured by GEOS-2 give no significant values for the phase differences because of the poor coherency in the pc5 period range.

We can estimate the amplitude, $b_\perp$, of the transverse magnetic field oscillation by the expression

$$b_\perp = \mu_0 e \delta N_h l \omega_D / k_\perp \tag{11}$$

(cf. Kremser et al., 1981), where e = charge of protons and $2l$ = length of the magnetic bottle along the field line. The maximum amplitude of $b_\perp$ should occur at the ends of the magnetic bottle, not at the equator where the magnetic bottle is formed by the drift mirror instability. We use a value $N_h = \beta_\perp B^2 / 2\mu_0 T_\perp \simeq 1.5\ \mathrm{cm}^{-3}$, and for l we take the same value as used by Kremser et al. (1981), i.e. $l \simeq 10^4$ km. With these values and the relation $\delta N_h \simeq 0.4 N_h$, we obtain $b_\perp \simeq 5$ nT. Note that we have ignored the reflection of the Alfvén wave at the ionosphere. Nevertheless, this transverse wave will not be seen on the ground because of ionospheric shielding. The value of $b_\perp$ just above the ionosphere will be reduced by a factor $g = (\Sigma_H / 2\Sigma_P) \exp(-x|k_\perp| h)$ when the signal reaches the ground (e.g. Glaßmeier, 1984). Here Σ_H and Σ_P are the height-integrated Hall and Pedersen conductivities, x is the reduction factor of the scale lengths mapped from the equatorial plane down to the ionosphere and h is of the order of 120 km. If we substitute $\Sigma_H / \Sigma_P \simeq 2$ and $x \simeq 15$, we obtain $g \simeq 10^{-3}$, i.e. the amplitude of a shear Alfvén wave coupled to the drift mirror mode is less than 0.1 nT at the ground.

The shape of E_φ agrees well with the shape of H-MAR, and E_φ leads H-MAR by $50° \pm 10°$ (period ~ 300 s). During the pc5 event starting around 1200 UT, E_φ reaches an amplitude of 5 mV/m peak-to-peak and E_φ leads E_v in phase by $\sim 10°$.

Walker et al. (1982, 1983) studied a similar event which also occurred in the early afternoon sector. They also found that B_φ leads B_μ in phase by $\sim 90°$. However, B_v and B_μ were in phase, in contrast to our observation where they are in anti-phase. Note that Walker et al. (1982) obtained an excellent peak-to-peak correlation between the three magnetic field components measured on board GEOS-2 (see their Fig. 2). The amplitude ratio of the components B_v (corresponding to the guided poloidal mode of a standing Alfvén wave) and B_μ (corresponding to the compressional wave) was ~ 0.3 for the event analysed by Walker et al. (1982). In our case both amplitudes do not differ very much (see Fig. 6). The theory of the coupling between a drift mirror wave and a standing Alfvén wave developed by Walker et al. (1982) predicts that B_μ, E_v and E_φ have antinodes at the equator, and B_φ, B_v have nodes. Therefore, B_v should be much smaller than B_μ at the position of GEOS-2. In the extended study, Walker et al. (1983) found that the drift mirror wave they observed was symmetric about the equator and was coupled to a second-harmonic standing Alfvén wave (poloidal mode, antisymmetric about the equator, E_φ lagged B_v by $\sim 90°$), which could not be explained by the theory.

According to Walker et al. (1982) the oscillations in B_μ, B_φ and E_v belong to the drift mirror wave, while the oscillations in B_v and E_φ represent the guided poloidal mode. We can estimate the amplitude of E_v from

$$E_v = \frac{\omega_D}{k_\perp} B_\mu \tag{12}$$

(Walker et al., 1982). If we substitute $B_\mu \simeq 30$ nT, we obtain $E_v \simeq 0.1$ mV/m, which is below the detection level of the GEOS-2 instrument.

The wave field data from GEOS-2 allow an estimation of the Poynting flux **S**. The three components are displayed in Fig. 7. What stands out clearly are the predominantly negative values of S_φ between ~ 1140 and 1152 UT, i.e. at the time of the largest variations of B_μ and the occurrence of the pc2 wave packets. At the same time, negative values dominate in the S_μ component. A negative value of S_φ indicates a westward Poynting flux (in the direction of the gradient-B drift of ions), while $-S_\mu$ means a southward flux (towards the ionosphere). In contrast to this, at the time of the small pc5 event starting around 1201 UT, positive values of S_φ and negative values of S_v probably dominate. It would indicate an eastward and inward-directed aver-

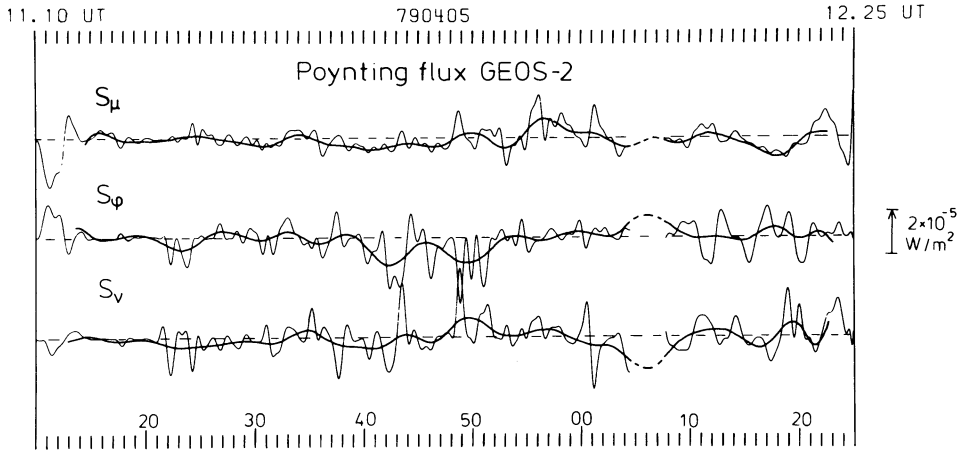

Fig. 7. Poynting flux given in the three components S_μ, S_φ and S_v. Bandpass-filtered data (cut-off periods 60 and 600 s) are used for the calculations. Low pass filtered traces (cut-off period 300 s) are also shown to recognize deviations from the mean values (*dashed lines*)

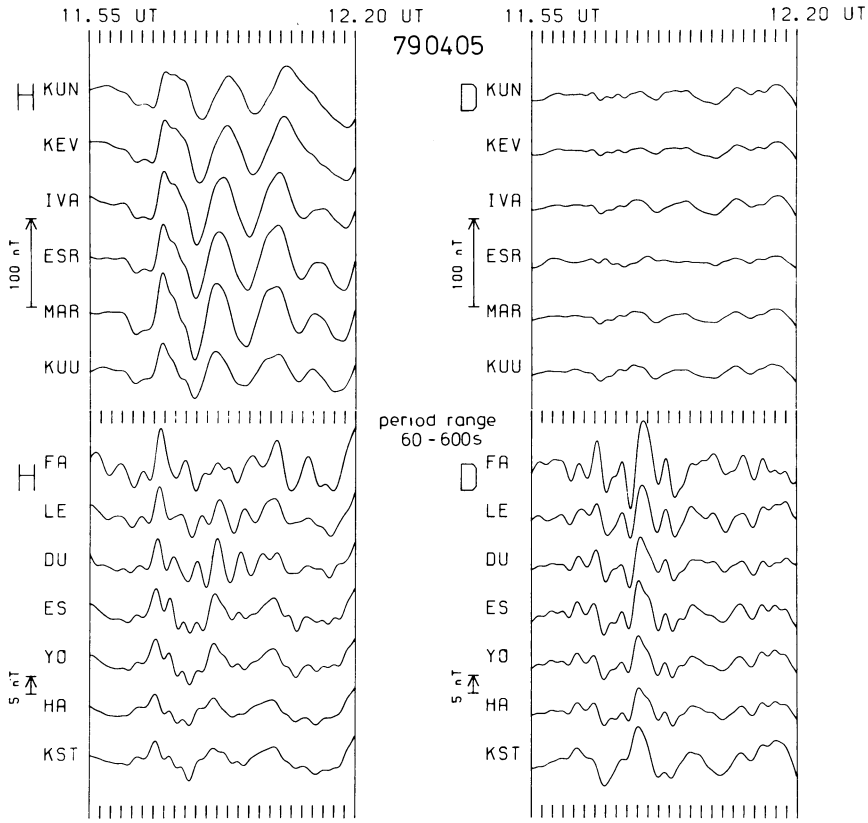

Fig. 8. Bandpass-filtered data from 13 European magnetometer stations. The records are arranged by geomagnetic latitude. Note the four times larger scale factor belonging to the Middle European stations

aged Poynting flux. This feature is consistent with a solar wind driven surface wave on the outer boundaries of the magnetosphere, which couples into a resonant shear Alfvén wave inside the *L*-shell passing through GEOS-2 (cf. Junginger, 1984). We have to examine the ground-based observations to support the assumption of a field line resonance phenomenon.

Ground-based observations. Figure 8 shows the filtered data (60–600 s) from 13 European stations for the time interval 1155–1220 UT. In northern Scandinavia the pc5 event with a period of ~300 s only appears in the *H* component, and the maximum of 100 nT peak-to-peak occurs far to the south at MAR ($L=5.1$). At the mid-latitude stations, HA ($L=2.4$) and KST ($L=2.3$), the amplitudes still exceed ~7 nT peak-to-peak in *H*. In Scandinavia the phase changes systematically from south to north (by ~75° between *H*-KUU and *H*-KUN) and from west to east (by ~17° between *H*-ESR and *H*-IVA). For the azimuthal wave number *m* we obtain $m=3$. This value supports the Kelvin-Helmholtz instability as a source of the pulsation energy (cf. Rostoker et al., 1980).

Along the U.K. chain the period of ~300 s is visible in *H* and *D* at all stations and *H*-HA leads *H*-FA in phase by ~40°. The sense of polarization in the $H-D$ plane is counter-clockwise at all stations in Middle Europe and approximately linear at the Scandinavian stations. Only the three northernmost stations (north of the amplitude maximum region) indicate a small ellipticity with a clockwise sense of polarization. Such a distribution of the polarization pattern is expected for a

field line resonance triggered by a Kelvin-Helmholtz instability in the morning sector (Chen and Hasegawa, 1974; Southwood, 1974), but the time is about 1500 MLT.

Power spectra, estimated from the time interval 1200–1218 UT, show two other spectral peaks in the pc4 period range at 120 and 75 s. The period of 120 s is dominating in the H component and shows amplitude maxima at KEV ($L=6.0$) and DU ($L=3.5$). The period of 75 s dominates in the D component at all stations except the sites between $L=4.6$ and 5.5 where the H component shows the spectral peak. Amplitude maxima are found in H-MAR ($L=5.1$) and D-ES ($L=2.9$). Again H-ESR leads H-IVA in phase by $\sim 16°$. The pc4 event with the shorter period (75 s) shows a polarization pattern similar to that of the pc5 event. The reversal of the sense of polarization occurs between the Scandinavian and the Middle European stations. For the period of 120 s the polarization pattern is not very clear.

The pc4 events show a stronger variation of the phase with latitude for the U.K. chain than for the Scandinavian chain, with the southern stations leading in phase. The phase of the pc4 event with period 120 s (75 s) changes by $\sim 160°$ ($\sim 100°$) between the H component of HA and FA.

The pc5 event is not visible in the STARE data (not shown), probably because of the threshold which the ionospheric electric field has to exceed to permit the development of radar auroral irregularities (cf. Walker et al., 1982). Between 1120 and 1220 UT, STARE detected only some patches of a northward-directed electric field, mainly north of Scandinavia, and not well correlated with the pulsation events.

In North America the pc5 event is also visible with small amplitudes below 30 nT and a similar period.

Short-period waves

Between 1115 and 1220 UT ion cyclotron waves were recorded on GEOS-2. Figure 9 shows the spectral density of the ULF waves in the frequency range 0.0–1.5 Hz from 1100 to 1230 UT. The ion cyclotron waves with frequencies just above the He^+ gyrofrequency have amplitude maxima at times of minima in the He^+ gyrofrequency. The broadband noise starting around 1225 UT is associated with the onset of the si.

The proton cyclotron waves are not seen as pc1 events in the sonograms of the search coil magnetometer station at Sodankylä (T. Bösinger, pers. comm.). The left-hand-polarized component, *BL*, also indicates some spectral energy near 0.1 Hz starting around 1135 UT. This corresponds to the pc2 events seen on the ground. These pc2 wave packets are interpreted as O^+ cyclotron waves (cf. Inhester et al., 1984). The abundance of O^+ ions in the magnetosphere prevents the proton cyclotron waves penetrating from the equatorial plane to the ionosphere (cf. Perraut et al., 1984).

The fact that the pc1–2 wave activity occurs during B_μ minima supports the conception of a mirror mode where the ions are driven out of the region of B_μ maxima by the mirror force. The largest ion temperature anisotropy is hence found in the region of B_μ minima and exists there as an energy reservoir for the pc1–2 waves. However, the usual theory of ion cyclotron wave generation that assumes a homogeneous medium can, apparently, not be applied in this case because of the small perpendicular wavelength of the hydromagnetic wave in which the pc1–2 waves are embedded.

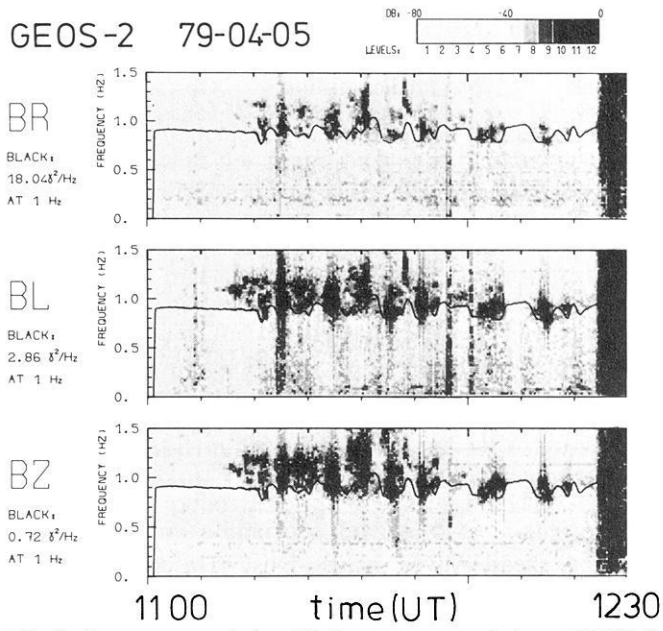

Fig. 9. Sonograms of the ULF waves recorded at GEOS-2 and separated into the right-handed (*BR*) and left-handed (*BL*) polarized and the field-aligned components. The *continuous solid line* gives the He^+ gyrofrequency computed from the fluxgate magnetometer data

Magnetosonic waves, not visible on the sonograms presented here, also occur between about 1145 and 1220 UT. Their frequencies are above the proton gyrofrequency and they are strongly polarized along the magnetic field **B**, implying a propagation in a direction almost perpendicular to **B** (Perraut et al., 1982).

Summary and discussion

Drift mirror instability and associated waves

The events between 1121 and 1225 UT observed in the afternoon sector are essentially controlled by drifting energetic ions injected on the nightside in connection with a substorm expansion phase. At the position of the geostationary satellite GEOS-2, $\beta_\perp$ increased to values between 0.1 and 0.5, while the ratio of the ion temperatures $T_\perp/T_\parallel$ varied between ~ 1.3 and 2. At geostationary orbit, strong wave-particle interactions are observed: we assume a drift mirror wave (pc5, about 3 mHz) associated with oxygen cyclotron waves (pc2, about 0.1 Hz), proton cyclotron waves (pc1, about 1.2 Hz), and magnetosonic waves (about 5 Hz). The three types of waves below the proton gyrofrequency are unstable in the case of relatively dense and highly anisotropic ion distributions with large perpendicular energies.

In a high-β inhomogeneous magnetospheric plasma composed of cold and hot components, only the drift mirror instability, the drift compressional instability

Table 2. Comparison of some predicted and observed quantities

Physical quantity	Predictions for drift mirror instability	Observed values
Phase difference, B and $\bar{J}$	180°	180°
$dJ_e/d\alpha$	$\gtrless 0$ for $\alpha \gtrless 90°$	$\gtrless 0$ for $\alpha \gtrless 90°$
$\beta_\perp$	$\cong 1$	0.1–0.5
$A=(T_\perp/T_\parallel)-1$	$\cong 1$	0.3–1.0
$k_\perp \rho_i$	$\cong 1$	$\cong 0.38$
ω_D	$\cong 0.019\ s^{-1}$ [a]	$\cong 0.003$–$0.019\ s^{-1}$
$P_\perp/P_\parallel$	$\cong 3$ [a]	$\gtrsim 10$
$b_\parallel$	$\simeq 80$ nT [a]	$\simeq 25$ nT

[a] These values are calculated according to Hasegawa's (1969) theory using other observed values

and the shear Alfvén waves exist (Hasegawa, 1975). According to Lin and Parks (1978), the ratio of the hot particle density to the total particle density, N_h/N, should not exceed a value of 0.01 to excite a drift compressional instability assuming an anisotropy $A \simeq 0.6$ found in our case. We estimated $N_h/N \gtrsim 0.1$, i.e. the drift compressional instability will play no role in our case.

We assume the occurrence of a drift mirror instability, although the estimated parameters do not fully reach the instability condition given by Hasegawa (1969). Nevertheless, Hasegawa (1969) developed a linear theory which ignores a multispecies plasma and the coupling between drift mirror and shear Alfvén modes.

We have shown that westward-drifting ion bunches passed GEOS-2. The westward propagation of the drift mirror wave is supported by a westward-directed Poynting flux at the position of GEOS-2 during a pronounced time interval. The observed diamagnetic drift in the opposite direction, which is only an apparent drift, obviously plays no important role in our case. In Table 2 the values of some parameters predicted by the model (Hasegawa, 1969; Lanzerotti et al., 1969) are compared with observed values. Note that the abundance of O^+ ions will probably reduce the predicted value of the frequency ω_D, leading to a closer agreement with the observations. ω_D and the observed frequency range are given in the stationary GSE-system.

We have shown that the wavelength of the disturbance in the equatorial plane ($\lambda_\perp$) is about 22 times the thermal ion gyroradius, ρ_i. For the event studied by Walker et al. (1982, 1983) $\lambda_\perp$ was nearly 25 times the gyroradius of 40 keV protons. Walker et al. (1982) therefore proposed that the eigenfrequency of the magnetic field line, $\omega_A = k_\parallel v_A$ (v_A = Alfvén velocity), also determines $k_\perp$, i.e. the wavelength corresponding to

$$k_\perp v_D = \omega_D \simeq \omega_A$$

grows fastest. This is a result of the boundary conditions forcing the Alfvén waves to produce a standing wave.

If we use the observed plasma density of $15\ cm^{-3}$ also for ions and split the number density into 85% protons and 15% O^+ ions (at 1200 UT $\sim 2.1\ cm^{-3}$ O^+ ions observed), we estimate an angular frequency $\omega_A \simeq 15 \times 10^{-3}\ s^{-1}$ (period ~ 420 s) for the fundamental toroidal mode of the L-shell passing through GEOS-2 (Orr and Matthew, 1971). This frequency decreases to $\sim 11 \times 10^{-3}\ s^{-1}$ for a fundamental poloidal mode. It is a value close to the estimated drift wave frequency, ω_D, and related to a parallel wavelength, $\lambda_\parallel \simeq 30 R_E$, about twice the length of the magnetic field line at $L=6.6$. Therefore, we obtain a ratio of the parallel to the perpendicular wave number $k_\parallel/k_\perp \simeq 10^{-2}$.

The coupling between drift and shear Alfvén modes was investigated by Patel and Migliuolo (1980) using a multispecies plasma model. They found that the coupling is weakened when an abundance of hot heavy ions (in particular O^+ ions) is present. This may happen also in our case, where the generation of O^+ cyclotron waves proves the presence of a certain amount of energetic O^+ ions.

Also in the case of a strong coupling we are not able to observe transverse pc5 waves related to the drift mirror wave (and having the same perpendicular wave number) at the ground-based magnetometer stations. They are screened by the ionosphere because of the short perpendicular wavelength (e.g. Glaßmeier, 1984).

The magnetic field components, B_v and B_φ, measured by GEOS-2 show a poor correlation with B_μ, while the electric field components indicate no significant correlation with B_μ.

We therefore assume a weak coupling between drift mirror and standing Alfvén waves.

In the model developed by Southwood (1977), the occurrence of wave structures where B_μ and B_v are 180° out of phase and B_φ is in quadrature with the larger component B_v is possible. Our observations are consistent with such a surface wave-like structure for which the Kelvin-Helmholtz instability may be the source of energy. The right-handed sense of polarization in the plane perpendicular to **B** observed in the afternoon sector (only for the polarized part of the magnetic signals) coincides with the assumption of a surface wave driven by the solar wind. Remember that GEOS-2 had entered the magnetopause boundary layer about 1 h before and probably rested in the vicinity of the magnetopause. We therefore may expect that the distance between GEOS-2 and the magnetopause was smaller than the azimuthal wavelength of a surface wave, i.e. if a surface wave was excited, GEOS-2 should most likely have observed its amplitudes (cf. Junginger, 1984). However, a coupling with the drift mirror wave seems to be unlikely because the **k**-vectors of both waves strongly differ in direction and magnitude.

Storm-associated pc5 pulsations with a similar magnetic field structure observed at synchronous orbit have, for example, been reported by Barfield and McPherron (1972). Lin and Parks (1978) found an agreement of these observations with their theory, where an "Alfvén-like wave" couples to the drift mirror instability. Our observations do not differ too much from the parameters used by Lin and Parks (1978) in one of the examples they calculated (see their Figs. 8 and 9). These calculations predict an amplitude ratio $B_v/B_\mu \lesssim 1$ and a 180° phase difference between these components, just as we observed it. Nevertheless, the degree of mode coupling remains an open question in our case.

The pc5 event starting around 1201 UT at the ground and in the electric field measured by GEOS-2 probably gets its energy from the solar wind. It is ultimately excited by a Kelvin-Helmholtz instability and shows no correlation with the drift mirror wave which exists at the same time. A compressional surface wave is generated either at the magnetopause or in the low-latitude boundary layer (LLBL). The fast mode propagates inwards and couples to the shear Alfvén wave of a local resonant field line (Chen and Hasegawa, 1974; Southwood, 1974). The drift mirror wave could also be triggered by the Kelvin-Helmholtz instability. In any case, this drift wave gets the energy mainly from the fields and particles of the near surroundings.

In northern Scandinavia the pc5 event is principally visible in the H component and the amplitude maximum occurs near $L=5$, i.e. at a very low latitude compared with the usually observed location of the resonance region for this frequency range. This event could be interpreted as a clear toroidal mode resonance, taking into account a 90° rotation of the magnetic polarization ellipse due to transmission through the ionosphere (e.g. Hughes, 1974). Near the footprint of the GEOS-2 magnetic field line, low cosmic noise absorption was detected starting around 1100 UT. The maximum absorption, reaching 1.2 dB, is seen at Ivalo ($L=5.5$) at 1115 UT (A. Ranta, pers. comm.). The precipitating electrons could change the ionospheric conductivity, and no full 90° rotation of the magnetic polarization ellipse would therefore be expected anymore because of a non-uniform ionosphere (e.g. Glaßmeier, 1984). Nevertheless, it is surprising that the amplitude of E_φ exceeds that of E_ν, indicating a dominant poloidal mode at GEOS-2.

The resonance region probably lies inside the L-shell passing through GEOS-2. Besides the position of the amplitude maximum, the probably eastward-directed Poynting flux supports this assumption. According to Junginger (1984), the azimuthal component of the Poynting vector is parallel to the **k**-vector of the surface wave between the magnetopause and the resonant L-shell and is antiparallel on the earthward side of the resonance region. Above the resonance region, E_ν decreases much faster with increasing L-value than E_φ (cf. Walker, 1980). We assume that the amplitude of E_ν has already fallen below the amplitude of E_φ at the position of GEOS-2.

According to Orr and Matthew (1971), the estimated period of ~ 420 s (see above) decreases to ~ 230 s if we move from $L=6.6$ to $L=5$ and assume a change of the ion density with the fourth power of the inverse radial distance from the earth. Therefore, the observed resonance near $L=5$ with a period of ~ 300 s should correspond to the fundamental toroidal mode.

The pc4 events with periods of 120 and 75 s occurred simultaneously with the large pc5 event. The first amplitude maximum was detected at high latitudes, suggesting a higher harmonic of the fundamental Alfvén wave. A secondary maximum in the middle of the U.K. chain leads to the assumption of further field line resonances in this region close to the plasmapause. The assumption is supported by the large phase changes across the maximum region.

Besides the phase changes, the eastward-directed apparent phase velocity detected at $L \simeq 5.5$ for the periods 300 and 75 s (calculated azimuthal wave number: $m=3$) is consistent with the assumption that the Kelvin-Helmholtz instability is involved in the generation of the pulsations. However, the polarization pattern (clockwise north of the amplitude maximum and counterclockwise at mid-latitudes) indicates a westward-directed **k**-vector of the surface wave at the magnetopause. This is expected for the morning sector. The magnetic local time (MLT) of the U.K. stations is ~ 1240 at 1200 UT, i.e. about 2 h earlier than the MLT of the Scandinavian stations. Therefore, the stations from FA to HA are still in the transition zone of morning and afternoon sector. Furthermore, the pc5 event shows a nearly linear polarization at the Scandinavian stations, and uncertainties due to influences of field-aligned currents and induction effects of the earth have to be taken into account. Perhaps several waves with similar frequencies but different energy sources are superimposed. Also in other papers, a confused behaviour in the sense of polarization in the post-noon sector is noted (cf. Rostoker et al., 1980).

Conclusions

For a special time interval, several types of pulsations have been analysed. Data were taken mainly from European stations and GEOS-2, covering the early afternoon sector.

The observations strongly support the assumption of a drift mirror instability detected by GEOS-2. The abundance of hot O^+ ions probably influenced the growth rate, the frequency of the drift mirror wave and the coupling between this wave and a shear Alfvén mode. This coupling and, therefore, also the amplitudes of flux and field variations detected by GEOS-2 are not fully understood and need further investigations. GEOS-2 was close to the magnetopause and perhaps strongly noticed its dynamic behaviour. For some parameters, only partial agreement between the observations and the predictions of Hasegawa's (1969) linear theory is found.

The parallel wavelength seems to be extremely short, indicated by a large ratio $P_\perp/P_\parallel$, much larger than predicted by the theory. Only the ions with pitch angles near 90° interact strongly with the drift mirror wave. On the other hand, the drift wave frequency is close to the frequency of a fundamental poloidal mode. If we assume a coupling between these modes we should obtain a very large parallel wavelength.

Pc4–5 events, detected on the ground and in the electric field measured by GEOS-2, seem to have a solar wind driven energy source (e.g. Kelvin-Helmholtz instability at the magnetopause or in the low-latitude boundary layer). The assumed field line resonances occurred at lower L-shells than the L-shell passing through GEOS-2. No coupling between these field line resonances and the drift mirror mode could be observed. It, also, is not expected because of different **k**-vectors of the waves. Only the polarization pattern

partly indicates a superposition of field line resonances and additional wave phenomena which may partly be related to the drift mirror instability.

Appendix

Equation (2) makes use of the fact that a spacecraft does not only measure the local properties of the plasma versus time; but due to the finite gyroradius of energetic particles, energy and azimuth angle variation of the particle flux allow the spatial structure of the surrounding plasma to be resolved also.

For a derivation of Eq. (2), we assume that the hydromagnetic wave only modulates the guiding centre density of the ion distribution, $F(\mathbf{r}, \mathbf{v})$, which we assume to be bi-Maxwellian. Then the perturbed part of F is

$$f = \frac{N(\mathbf{r}, \mathbf{v})}{(2\pi)^{3/2}} \frac{m_i^{3/2}}{T_\perp T_\parallel^{1/2}} e^{-\varepsilon \frac{(1 + A\cos^2\alpha)}{T_\perp}},$$

where $\varepsilon = m_i v^2/2$ is the energy, $A = (T_\perp/T_\parallel) - 1$ the temperature anisotropy and α the pitch angle. In a sinusoidal wave, the perturbed density is $N = \delta N_h \cos(\mathbf{k} \cdot \mathbf{R})$, where $\mathbf{R} = \mathbf{r} - (\hat{\mathbf{b}} \times \mathbf{v})/\Omega$ is the position of the guiding centre in terms of phase space coordinates and the unit vector $\hat{\mathbf{b}}$ along the magnetic field line. The flux density, j, per energy interval and phase space angle is

$$j d\varepsilon d\Omega = v f d^3 v = \frac{2}{m_i^2} \varepsilon f \sin\alpha d\varepsilon d\varphi d\alpha.$$

Here, both sides have the unit (counts/s m^2) and (φ, α) are to be taken as the azimuth and pitch angle of the observation direction.

During the wave maxima, we approximate $\cos^2\alpha = 1$ in f and the ion flux above a particle energy E for a fixed azimuth and pitch angle is given by

$$J_1 d\Omega = \frac{2\delta N_h \sin\alpha d\alpha d\varphi}{(2\pi)^{3/2} m_i^{1/2} T_\perp T_\parallel^{1/2}} \int_E^\infty d\varepsilon \varepsilon e^{-\varepsilon/T}.$$

Note, that SI units have to be used for the energy and temperature and $T = T_\perp/(1 + A\cos^2\alpha)$ is the effective ion temperature at a pitch angle α.

At the time of a wave node, we approximate $\cos(\mathbf{k} \cdot \mathbf{R}) = \mathbf{k} \cdot (\hat{\mathbf{b}} \times \mathbf{v})/\Omega = k_\perp v_\perp \sin(\varphi - \varphi')/\Omega$ where φ' is the azimuth angle of the wave vector. The maximum ion flux above the energy E is observed at an azimuth angle φ perpendicular to φ' and amounts to

$$J_2 d\Omega = \frac{2\delta N_h \sin\alpha d\alpha d\varphi}{(2\pi)^{3/2} m_i^{1/2} T_\perp T_\parallel^{1/2}} \sqrt{\frac{2}{m_i}} \frac{k_\perp \sin\alpha}{\Omega} \int_E^\infty d\varepsilon \varepsilon^{3/2} e^{-\varepsilon/T}.$$

A straightforward calculation of the integrals in the expressions for J_1 and J_2 yields the desired result. The approximations that were made for $\cos(\mathbf{k} \cdot \mathbf{R})$ are justified for the measurements discussed in the main text. Since there $E \cong T$, the relative error of the approximations is of the order of $k_\perp^2 T/\Omega m_i \cong 0.1$, which seems sufficient in view of the fact the actual wave form is not sinusoidal as has been assumed.

Acknowledgements. The authors are grateful to the many IMS groups who supported the work by making their data available. In particular, we thank G. Wrenn, E. Nielsen, H. Ranta, A. Ranta, B. Higel, S. Perraut, N. Cornilleau-Wehrlin, J. Etcheto, M. Stokholm, T. Bösinger, H. Maurer, M. Lester, C.T. Russell (ISEE-3 magnetometer data) and N.F. Ness (IMP-8 magnetometer data). The World Data Center A provided us with further information. Thanks are due to G. Wrenn who organized the Sixth Workshop on IMS Observations in Northern Europe at Cumberland Lodge, Windsor, and D. Orr who was an excellent convener of the pulsation group, strongly promoting this work. We also want to thank O. Hillebrand for selecting the special event some years ago and collecting and analysing a first data set.

The contribution by C.A.G. is published with the approval of the Director, Institute of Geological Sciences (NERC), UK. The German part of the ground magnetometer recordings has been financially supported by the Deutsche Forschungsgemeinschaft.

References

Barfield, J.N., McPherron, R.L.: Statistical characteristics of storm-associated Pc5 micropulsations observed at the synchronous equatorial orbit. J. Geophys. Res. **77**, 4720–4733, 1972

Brown, W.L., Cahill, L.J., Davis, L.R., McIlwain, C.E., Roberts, C.S.: Acceleration of trapped particles during a magnetic storm on April 18, 1965. J. Geophys. Res. **73**, 153–161, 1968

Chen, L., Hasegawa, A.: A theory of long-period magnetic pulsations, 1. Steady state excitation of field line resonance. J. Geophys. Res. **79**, 1024–1032, 1974

Geiss, J., Balsiger, H., Eberhardt, P., Walker, H.P., Weber, L., Young, D.T., Rosenbauer, H.: Dynamics of magnetospheric ion composition as observed by the GEOS mass spectrometer. Space Sci. Rev. **22**, 537–566, 1978

Gendrin, R.: Magnetic turbulence and diffusion processes in the magnetopause boundary layer. Geophys. Res. Lett. **10**, 769–771, 1983

Glaßmeier, K.-H.: On the influence of ionospheres with non-uniform conductivity distribution on hydromagnetic waves. J. Geophys. **54**, 125–137, 1984

Greenwald, R.A., Walker, A.D.M., Candidi, M.: Use of hydromagnetic waves to map geomagnetic field lines. J. Geophys. Res. **86**, 11251–11257, 1981

Gurgiolo, C., Lin, C.S., Mauk, B., Parks, G.K., McIlwain, C.: Plasma injection and diamagnetism. J. Geophys. Res. **84**, 2049–2056, 1979

Hasegawa, A.: Drift mirror instability in the magnetosphere. Phys. Fluids **12**, 2642–2650, 1969

Hasegawa, A.: Plasma instabilities and nonlinear effects. Berlin, Heidelberg, New York: Springer 1975

Hughes, W.J.: The effect of the atmosphere and ionosphere on long period magnetospheric micropulsations. Planet. Space Sci. **22**, 1157–1172, 1974

Inhester, B., Wedeken, U., Korth, A., Perraut, S., Stokholm, M.: Ground-satellite coordinated study of the April 5, 1979 events: Observation of O^+ cyclotron waves. J. Geophys., this issue, 1984

Junginger, H.: The Poynting vector of boundary surface waves and resonant shear Alfvén waves in a cold, inhomogeneous plasma. J. Geophys. Res., in press, 1984

Korth, A., Kremser, G., Wilken, B.: Observations of substorm-associated particle-flux variations at $6 \leqq L \leqq 8$ with GEOS-1. Space Sci. Rev. **22**, 501–509, 1978

Kremser, G., Korth, A., Fejer, J.A., Wilken, B., Gurevich, A.V., Amata, E.: Observations of quasi-periodic flux varia-

tions of energetic ions and electrons associated with Pc5 geomagnetic pulsations. J. Geophys. Res. **86**, 3345–3356, 1981

Lanzerotti, L.J., Hasegawa, A.: High β plasma instabilities and storm time geomagnetic pulsations. J. Geophys. Res. **80**, 1019–1022, 1975

Lanzerotti, L.J., Southwood, D.J.: Hydromagnetic waves. In: Solar system plasma physics, Vol. III, L.J. Lanzerotti, C.F. Kennel, E.N. Parker, eds.: pp. 109–135. Amsterdam: North-Holland 1979

Lanzerotti, L.J., Hasegawa, A., Maclennan, C.G.: Drift mirror instability in the magnetosphere: Particle and field oscillations and electron heating. J. Geophys. Res. **74**, 5565–5578, 1969

Lin, C.S., Parks, G.K.: The coupling of Alfvén and compressional waves. J. Geophys. Res. **83**, 2628–2636, 1978

McPherron, R.L.: Magnetospheric substorms. Rev. Geophys. Space Phys. **17**, 657–681, 1979

Montbriand, L.E.: A simple method for calculating the local time of corrected geomagnetic midnight. J. Geophys. Res. **75**, 5634–5636, 1970

Ng, P.H., Patel, V.L.: The importance of ∇B drift in high β magnetospheric plasma instabilities. Geophys. Res. Lett. **10**, 17–19, 1983

Orr, D., Matthew, J.A.D.: The variation of geomagnetic micropulsation periods with latitude and the plasmapause. Planet. Space Sci. **19**, 897–905, 1971

Patel, V.L., Migliuolo, S.: Alfvén waves and drift compressional modes in multispecies plasmas. J. Geophys. Res. **85**, 1736–1742, 1980

Patel, V.L., Ng, P.H., Cahill, L.J., Jr.: Drift wave model for geomagnetic pulsations in a high β plasma. J. Geophys. Res. **88**, 5677–5684, 1983

Pedersen, A., Grard, R.: Quasistatic electric field measurements on the GEOS-1 and GEOS-2 satellites. In: Quantitative modeling of magnetospheric processes, Monogr. Ser. **21**, W.P. Olson, ed.: pp. 281–296. Washington, D.C.: American Geophysical Union 1979

Perraut, S., Gendrin, R., Robert, P., Roux, A., de Villedary, C.: ULF waves observed with magnetic and electric sensors on GEOS-1. Space Sci. Rev. **22**, 347–369, 1978

Perraut, S., Roux, A., Robert, P., Gendrin, R., Sauvaud, J.-A., Bosqued, J.-M., Kremser, G., Korth, A.: A systematic study of ULF waves above f_{H^+} from GEOS 1 and 2 measurements and their relationships with proton ring distributions. J. Geophys. Res. **87**, 6219–6236, 1982

Perraut, S., Gendrin, R., Roux, A., de Villedary, C.: Ion cyclotron waves: Direct comparison between ground-based measurements and observations in the source region. J. Geophys. Res. **89**, 195–202, 1984

Rostoker, G.: Triggering of expansive phase intensifications of magnetospheric substorms by northward turnings of the interplanetary magnetic field. J. Geophys. Res. **88**, 6981–6993, 1983

Rostoker, G., Samson, J.C., Olson, J.V.: Latitudinal and longitudinal variation of Pc4, 5 pulsations and implications regarding source mechanisms. J. Geomagn. Geoelectr. **32**, Suppl. II, SII 1-SII 15, 1980

Roux, A., Perraut, S., Rauch, J.L., de Villedary, C., Kremser, G., Korth, A., Young, D.T.: Wave-particle interactions near Ω_{He^+} observed on board GEOS 1 and 2, 2. Generation of ion cyclotron waves and heating of He^+ ions. J. Geophys. Res. **87**, 8174–8190, 1982

Russell, C.T., Southwood, D.J., eds.: The IMS Source Book. Washington, D.C.: American Geophysical Union 1982

Sonnerup, B.U.Ö., Cahill, L.J., Jr., Davis, L.R.: Resonant vibration of the magnetosphere observed from Explorer 26. J. Geophys. Res. **74**, 2276–2288, 1969

Southwood, D.J.: Some features of field line resonances in the magnetosphere. Planet. Space Sci. **22**, 481–491, 1974

Southwood, D.J.: Localised compressional hydromagnetic waves in the magnetospheric ring current. Planet. Space Sci. **25**, 549–554, 1977

Southwood, D.J., Hughes, W.J.: Theory of hydromagnetic waves in the magnetosphere. Space Sci. Rev. **35**, 301–366, 1983

Walker, A.D.M.: Modelling of pc5 pulsation structure in the magnetosphere. Planet. Space Sci. **28**, 213–223, 1980

Walker, A.D.M., Greenwald, R.A., Korth, A., Kremser, G.: STARE and GEOS 2 observations of a storm time Pc5 ULF pulsation. J. Geophys. Res. **87**, 9135–9146, 1982

Walker, A.D.M., Junginger, H., Bauer, O.H.: GEOS 2 plasma drift velocity measurements associated with a storm time Pc5 pulsation. Geophys. Res. Lett. **10**, 757–760, 1983

Received November 7, 1983; Revised June 4, 1984
Accepted June 4, 1984